Samples

The materials for all the samples except tin No. 3 were purchased from United Mineral and Chemical Corporation in powder form with particle size less than 325 mesh (43-μ mesh). Although 43 μ exceeds the skin depth at 77°K, this introduces no distortion of the value of T_1 when the measurements are performed with a phase-coherent pulsed spectrometer, as has been shown theoretically[26] and has been verified experimentally.[26,31] The stated purities were 99.9999%; all materials were of natural isotopic abundance. All samples were sealed in 10-mm i.d., 12-mm o.d. Pyrex tubes. The details of making each sample are different and are given below.

Cadmium. The powder was mixed with an equal volume of silica powder, also less than 325 mesh, placed in the Pyrex tube, evacuated, and sealed with an argon atmosphere enclosed.

Tin No. 1. The tin sample was made by oxidizing the powder in an open test tube in an oven at 200°C for about 8 h. In this way the powder became covered with a durable oxide layer. The powder was then poured into a sample tube, evacuated, and sealed with an argon atmosphere enclosed. The sample was heated to ≈360°C (≈128°C above the melting point of tin); the powder still flowed freely.

Tin No. 2. From the same supply of powder as tin No. 1, the powder was mixed with 325-mesh quartz powder in a 50-50% mixture and placed in an unevacuated tube.

Tin No. 3. This sample was made from 200-mesh powder of 99.9% purity obtained from A. D. MacKay Co., New York. Otherwise this sample is identical to tin No. 2.

[31] D. F. Holcomb, J. A. Kaeck, and J. H. Strange, Phys. Rev. **150**, 306 (1966).

PHYSICAL REVIEW VOLUME 184, NUMBER 2 10 AUGUST 1969

Time-Differential Perturbed Angular-Correlation Experiment for ^{57}Fe in a Ni Host, and a Comparison with the Mössbauer Effect*

C. HOHENEMSER, R. RENO, H. C. BENSKI, AND J. LEHR†
Department of Physics, Brandeis University, Waltham, Massachusetts 02154
(Received 20 March 1969)

The 122–14-keV γ-γ cascade in ^{57}Fe has been used to detect the precession of the 14-keV state in the hyperfine field produced by a Ni lattice at ^{57}Fe impurity sites. The time-differential perturbed angular-correlation technique was used. The data yield a hyperfine field of -267.5 ± 2.7 kG at room temperature. The magnitude is in agreement with Mössbauer measurements; the sign is determined here for the first time. The data also yield a half-life of 99.3 ± 0.5 nsec for the 14-keV state, and an anisotropy coefficient $A_2=-0.0187\pm0.0015$ for the 122–14-keV cascade. In addition, the data show the absence of time-dependent perturbations over the experimental time interval of 400 nsec. Based on this, application to the study of critical field fluctuations is discussed.

1. INTRODUCTION

TIME-DIFFERENTIAL perturbed angular correlation (TDPAC) was originally used to measure magnetic moments of relatively long-lived (10–1000 nsec) excited states of nuclei by use of known applied fields. The technique consists essentially of a delayed coincidence measurement on a nuclear γ-ray cascade, in which the Larmor precession of the intermediate-state nucleus in the applied field is directly observed as oscillations on the lifetime curve. An excellent early example of such measurements is the work of Matthias *et al.*[1] on ^{111}Cd and ^{181}Ta. It can be seen from this, as well as more recent cases,[2,3] that among perturbed angular-correlation methods, TDPAC is at once the most precise and the most clearly interpretable. A possible exception is resonance destruction of angular correlations.[4]

In the last few years, TDPAC has been applied to internal fields at impurity nuclei in ferromagnetic hosts. In this role, TDPAC yields field values if the excited-state moment has been independently measured. Unlike nuclear magnetic resonance, and like Mössbauer and nuclear polarization experiments, TDPAC is very sensitive (impurity concentrations of 10^{-5} or better are typical) and does not suffer from rf absorption difficulties. TDPAC is potentially superior to Mössbauer experiments for low fields because a number of cascades have sensitivities of ~100 G,[5] while the best Mössbauer

* Work supported in part by the U. S. Atomic Energy Commission.
† Brandeis University Undergraduate Research Participant.
[1] E. Matthias, L. Boström, A. Maciel, M. Salomon, and T. Lindqvist, Nucl. Phys. **40**, 656 (1962).
[2] *Perturbed Angular Correlations*, edited by E. Karlsson, E. Matthias, and K. Siegbahn (North-Holland Publishing Co., Amsterdam, 1964).
[3] *Hyperfine Structure and Nuclear Radiations*, edited by E. Matthias and D. A. Shirley (North-Holland Publishing Co., Amsterdam, 1968).
[4] E. Matthias, D. A. Shirley, N. Edelstein, H. J. Körner, and B. A. Olsen, Ref. 3, p. 878.
[5] J. Alonso and L. Grodzins, Ref. 3, p. 549.

experiments have been limited to fields of $\sim$10 000 G or more. Despite its apparent advantages, TDPAC has yielded relatively few results on hyperfine fields.[6]

The principal difficulty with widespread application of TDPAC as an impurity field probe has been in the various shortcomings of the delayed coincidence technique, in particular, poor time resolution. Many interesting nuclear cascades (long intermediate-state lifetime, large anisotropy) involve low-energy γ rays, and the need to resolve energy to avoid interfering cascades. This has usually meant the use of NaI(Tl) scintillation counters, if not solid-state detectors, and has ruled out fast plastic scintillators in most cases. On the other hand, Larmor periods in interesting magnetic systems are most often in the region of 50 nsec or less, and require time resolution of 5 nsec or less, a condition which in the past could not often be met simultaneously with the energy resolution of the γ rays.

In this paper, we report on the first TDPAC measurement using the 14-keV state of ^{57}Fe. Our measurement on a Ni host was made possible largely by improved time resolution at low energy. It allows for an interesting comparison to the Mössbauer technique, which in the case of the 14-keV state of ^{57}Fe has been applied in literally hundreds of cases. Our experiment, as will become clear, has a sensitivity and accuracy comparable to the equivalent Mössbauer effect experiment. In addition, it allows a less ambiguous interpretation in regard to possible relaxation processes and multiple magnetic sites.

2. IMPROVED TIME RESOLUTION

Our experiment was made possible by considerable improvement in time resolution with NaI(Tl) at low energies. Before considering the data, we therefore discuss some aspects of the time resolution problem.

Recent progress in timing with NaI(Tl) is due to the advent of low-noise bialkali photocathodes in photomultipliers such as the RCA 8575. The low-noise characteristics of these photomultipliers were first exploited by Lynch,[7] who showed that by triggering timing discriminators at the level of single photoelectrons, the attainable resolutions with NaI(Tl) could be dramatically improved, particularly at low energy.

Lynch's results can be qualitatively understood if one visualizes the creation of a current pulse in the photomultiplier in the following way: (1) Visible photons, proportional in number to the γ energy loss E, are emitted with a mean life τ_s by the atoms of the scintillator; (2) the photons produce electrons at the photocathode with an efficiency of p electrons per keV; (3) the anode resistor passes a current $I(t)$ corresponding to the multiplication of the individual photoelectrons, with a dispersal in time of each photoelectron that corresponds to transit time differences through the multiplier. The current distribution due to a single electron is usually referred to as the single-electron response (SER). For very low energy the details of the SER are unimportant, the time between photoelectrons being as large or larger than the width of the SER. The time of rise of the anode pulse therefore reflects only the time of arrival of the first photoelectron at the anode. Assuming that there is no significant buildup time of optical excitations in the scintillator, the root-mean-square time of arrival of the first electron is, to first order,

$$\langle \Delta t_1 \rangle_{\rm rms} = \tau_s / pE. \tag{1}$$

On the other hand, the root-mean-square time of arrival of the second electron is, to first order,

$$\langle \Delta t_2 \rangle_{\rm rms} = \sqrt{2}\tau_s / pE. \tag{2}$$

These expressions follow from the formulation of Post and Schiff,[8] who ignore the SER entirely. While the expressions for $\langle \Delta t_1 \rangle_{\rm rms}$ and $\langle \Delta t_2 \rangle_{\rm rms}$ are strictly correct at *very* low energy, they are nevertheless a good measure of the time resolution that can be achieved at finite low energy, and they indicate the great importance of triggering the timing discriminators at the single-electron level for optimum timing. Lynch found that $p \simeq 8$ by analyzing his data by means of the Post-Schiff formulation. Houdayer *et al.*[9] obtain $p \simeq 10$ by a direct charge measurement. We have measured somewhat lower values which vary with crystal size and reach a maximum of $p \simeq 6$.

Before the advent of the RCA 8575, triggering at the level of a single photoelectron was made difficult if not impossible by the high dark noise of available photomultipliers. For example, in 1963, Weisberg[10] of this laboratory, while achieving resolution at high energy in plastic that still is essentially unsurpassed, measured $\sim$30 nsec full width at half-maximum (FWHM) with two NaI counters running at 30-keV energy loss. For 630–30-keV electron–γ-ray coincidences from ^{137}Cs, with the former detected in plastic, the Weisberg result would be $\sim$20 nsec FWHM. Lynch, using just such a setup, has measured a 2.0-nsec FWHM.

We have confirmed and extended Lynch's findings and have explained qualitatively the energy dependence of the resolution.[11] We have also shown that the excellent low energy resolution obtained with submicrocurie sources can be extended to the region of fairly high counting rates encountered in a practical TDPAC experiment. Thus, to achieve a coincidence rate of 50/sec in the experiment reported in this paper, we found, even with optimally thin crystals in the 14-keV detector, that the singles rate at the one-electron level was $\sim 10^5$ counts/sec. At such rates, the dark noise

[6] D. A. Shirley, Ref. 3, p. 979.
[7] F. J. Lynch, IEEE Trans. Nucl. Sci. **NS-13**, 140 (1966).
[8] R. F. Post and L. I. Schiff, Phys. Rev. **80**, 1113 (1950).
[9] A. Houdayer, S. K. Mark, and R. E. Bell, Nucl. Instr. Methods **59**, 293 (1967).
[10] H. Weisberg, Ph.D. thesis, Brandeis University, 1965 (unpublished).
[11] C. Hohenemser and R. Reno (to be published).

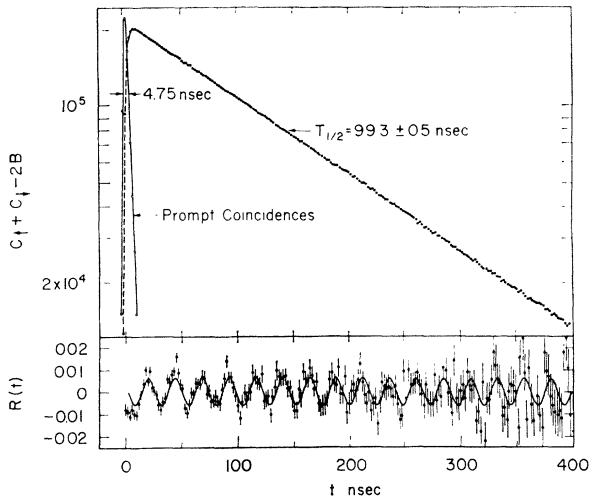

FIG. 1. Upper graph: Background-corrected 14-keV lifetime curve obtained by summing the data point by point, for applied field up and down. This removes the precession oscillations. The upper graph also shows the time resolution of the system, as obtained by direct measurement of 14–120-keV x-ray–γ-ray prompt coincidences from ^{88}Y. Lower graph: Dimensionless ratio $R(t)$, defined by Eq. (3) of the text. It exhibits constant-amplitude sinusoidal oscillations having twice the Larmor frequency. The solid line represents a least-squares fit to $R(t)$, as explained in the text.

pulses form only a small part of the detected events, and multiple triggerings from a single γ ray predominate. For this reason we introduced a sharply defined dead time following each discriminator triggering in order to reduce pileup that in effect ruins the time resolution and makes the accidental rate time-dependent. For the 14-keV detector this precaution proved sufficient. For the 122-keV detector, even with dead time of 2 μsec, the trigger rate at the one-electron level approached 10^6 counts/sec. It was therefore necessary to back off to the second or third electron level. Fortunately, at 122 keV this does not, as it does at very low energy, drastically reduce the time resolution, since one is here in a region of strongly overlapping SER's. With a 2.5×2.5-cm crystal for the 122-keV detector, and a 2.5×0.1-cm crystal for the 14-keV detector, with third electron and first electron triggering, respectively, and fast trigger rates of $\sim5\times10^4$ counts/sec in both channels, the measured time resolution, using a source of ^{88}Y, was 4.75 nsec.

The electronics employed in our experiment was otherwise a standard slow-fast arrangement, employing an ORTEC model 437 time-to-amplitude converter, and a 512-channel multichannel analyzer. The over-all system linearity was ~0.1%. The time calibration was achieved with a 10-MHz crystal clock, which provided correlated start and stop signals to the time-to-amplitude converter. This method is free of systematic errors that beset most time-calibration techniques, and accounts in part for the accuracy of the results obtained.

3. SOURCE AND GEOMETRY

The 4.0-μCi source for the experiment was produced by diffusion of ^{57}Co into a 0.0025-cm-thick Ni foil at 1000°C in a H_2 atmosphere, with subsequent vacuum annealing at 700°C to remove the H_2. The diffusion time was held to less than $\frac{1}{2}$h to minimize the absorption of the 14-keV γ rays in the source foil. The source foil was then magnetized to saturation by a small, reversible C-type electromagnet, across whose poles the source was clamped. The air-gap field of the magnet was 300 G. The saturation was directly checked by bulk magnetization measurements on the foil with a ballistic galvanometer. These measurements showed a magnetization equivalent to 0.60 magnetons per atom to within an experimental error of 10%.

The counters were set in a horizontal plane, and the magnet was arranged so that the direction of magnetization was perpendicular to the plane of the counters. For successive γ rays, with propagation vectors $\mathbf{k}_1$ and $\mathbf{k}_2$ lying in the xy plane, and a transverse magnetic field of magnitude H in the $+z$ direction of a right-handed coordinate system, the precession of the directional correlation function can be written[12]

$$W(\theta,t,H)=1+\sum_{N=2}^{k_{\max}} b_N \cos N(\theta-\omega_H t), \qquad (3)$$

where $\theta=\theta_2-\theta_1$, and θ_1 and θ_2 are the aximuthal angles of $\mathbf{k}_1$ and $\mathbf{k}_2$, respectively, and where $\omega_H=-g\mu_N H/\hbar$ is the Larmor frequency.

In our experiment, θ was $5\pi/4$ in a laboratory coordinate system in which the $+z$ axis is physically up. We measured coincidence rates $C_\uparrow(t)$ and $C_\downarrow(t)$, where $\uparrow$ and $\downarrow$ denote source-foil magnetization parallel and antiparallel to the $+z$ axis. The experimental counting rate is expected to be related to the correlation function by

$$C(t)=\text{const}e^{-t/\tau}W(t)+B, \qquad (4)$$

where τ is the mean life of the intermediate state and B is the time-independent background. It is natural to form the τ-independent, dimensionless ratio

$$R(t)\equiv[C_\downarrow(t)-C_\uparrow(t)]/[C_\downarrow(t)+C_\uparrow(t)-2B], \qquad (5)$$

which, under the assumption that *the hyperfine field H is antiparallel to the external field*, is given in terms of $W(t)$ by

$$R(t)=\frac{W(5\pi/4,t,H)-W(5\pi/4,t,-H)}{W(5\pi/4,t,H)+W(5\pi/4,t,-H)}. \qquad (6)$$

To first order in the sum of Eq. (1), this reduces to $b_2\sin2(-g\mu_N|H|t/\hbar)$. In an actual measurement, we may in fact expect that

$$R(t)=\gamma_a\gamma_t b_2\sin2(-g\mu_N|H|t/\hbar), \qquad (7)$$

[12] R. M. Steffen and H. Frauenfelder, Ref. 2, p. 3.

where γ_a and γ_t describe the attenuation due to finite angular and time resolution, respectively.

4. MEASURED FIELD

The experimental data in the form of Eq. (3) are shown in Fig. 1. To exhibit the frequency content of the data, we performed the Fourier transformation

$$F^2(\nu)=\left(\int R(t)\sin 2\pi\nu t\,dt\right)^2+\left(\int R(t)\cos 2\pi\nu t\,dt\right)^2 \quad (8)$$

and plotted it in Fig. 2. This form, which is independent of the choice of $t=0$, is, except for details of the line shape, equivalent to a nuclear-magnetic-resonance line, and indicates that $2\nu_H=42.1\pm0.5$ MHz. By use of the known g factor of the 14-keV state,[13] we calculate that the hyperfine field at room temperature has a magnitude of $|H|=267.8\pm2.7$ kG, where we neglect the applied field. This is in good agreement with the Mössbauer measurements of Wertheim[14] and of Dash, Dunlap, and Howard,[15] who obtain $|H|=265\pm5$ kG.

The sign of the hyperfine field is determined from the phase of $R(t)$ at $t=0$ in the following way: b_2 is negative,[16] $-g\mu_N|H|/\hbar$ is positive since g is negative, and hence $R(t)$, as given by Eqs. (4) and (5), should be negative going at the origin. Since this is what one observes, we conclude that H is indeed antiparallel to the source-foil magnetization, as assumed. [A positive-going $R(0)$ would imply a positive hyperfine field.] The negative sign for Fe in Ni has not been previously observed, but is in agreement with systematics discussed by Shirley and others.[17–19] With the sign of hyperfine field known, we may correct for the applied field, albeit trivially, and obtain $H=-267.5\pm2.7$ kG.

5. NUCLEAR PARAMETERS

In Fig. 1 we have also plotted $C_\uparrow(t)+C_\downarrow(t)-2B$, and since this is expected to be of the form $e^{-t/\tau}$, with the precession oscillations removed, we obtain a value of the half-life of the 14-keV state from it. The accidental background per channel B was calculated from the measured singles rates N_{14} and N_{122} by the relation

$$B=c_B T_l N_{14} N_{122}, \quad (9)$$

where c_B is the time per channel and T_l is the live time of the experiment. The time independence of B, as well as the relation (9), was checked by a separate experiment using an arrangement where only accidental coincidences are possible (one source near each counter and a total shield between them). A least-squares fit to the data in Fig. 1 gave a half-life value of $T_{1/2}=50.66\pm0.06$ channels. The time-calibration factor c_B was determined by the technique mentioned in Sec. 3, and led to the result

$$T_{1/2}=99.3\pm0.5 \text{ nsec}. \quad (10)$$

Thus, the uncertainty in $T_{1/2}$ is due largely to the systematic uncertainty in c_B. This, however, is *not* due to the oscillator stability or accuracy ($\leq 1\times10^{-5}$), but arises from the inability to locate exactly a time "spike" in a single channel ($<5\times10^{-3}$). Our half-life value agrees well with the two most recent results: 98.0 ± 1.0[20] and 97.7 ± 0.2 nsec.[21]

The solid curve in Fig. 1 shows a least-squared fit to the dimensionless ratio $R(t)$, in which the amplitude of the sine curve is treated as a parameter. The resulting value for the amplitude is $|\gamma_t\gamma_a b_2|=0.0071\pm0.0004$. By folding the time resolution in Fig. 1 into a sine wave of frequency $2\nu_H$, we obtain the attenuation factor due to time resolution $\gamma_t=0.74\pm0.02$. From analysis of the counter geometry and counter efficiencies[22] we obtain the angular attenuation factor $\gamma_a=0.69\pm0.02$. We therefore conclude that $b_2=-0.0140\pm0.0012$ or, in terms of the usual notation,

$$A_2\simeq\tfrac{4}{3}b_2=-0.0187\pm0.0015. \quad (11)$$

This should be compared to the result of Lindqvist and Heer,[16] who obtained $A_2=-0.024\pm0.003$. In our quoted result for A_2, we depend on Ref. 16 for the sign of A_2, as we did previously in deducing the sign of H. Strictly speaking, we have shown only that $A_2H>0$.

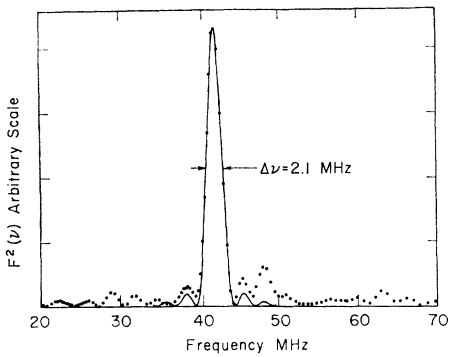

FIG. 2. Fourier transform of $R(t)$, as defined by Eq. (8) of the text. The solid line represents the expected line shape if $R(t)$ is given by an error-free sine wave over the interval of 400 nsec. The observed resonance frequency is interpreted as twice the Larmor frequency.

[13] V. S. Shirley, Ref. 3, p. 985.
[14] G. K. Wertheim, J. Appl. Phys. Suppl. **32**, 110S (1961).
[15] J. G. Dash, B. C. Dunlap, and D. G. Howard, Phys. Rev. **141**, 376 (1966).
[16] T. Lindqvist and E. Heer, Nucl. Phys. **2**, 280 (1956/57).
[17] D. A. Shirley and G. A. Westenbarger, Phys. Rev. **138**, A170 (1965).
[18] D. A. Shirley, S. S. Rosenblum, and E. Matthias, Phys. Rev. **170**, 363 (1968).
[19] D. A. Shirley, Ann. Rev. Nucl. Sci. **16**, 89 (1966).
[20] O. C. Kistner and A. W. Sunyar, Phys. Rev. **139**, B295 (1966).
[21] M. Eckhause, R. J. Harris, Jr., W. B. Shuler, and R. E. Welsh, Proc. Phys. Soc. (London) **89**, 187 (1966).
[22] M. J. L. Yates, in *Alpha-, Beta-, and Gamma-Ray Spectroscopy*, edited by K. Siegbahn (North-Holland Publishing Co., Amsterdam, 1966), p. 1691.

6. LINEWIDTH AND FLUCTUATIONS

The solid curve in Fig. 2 is the expected shape of $F^2(\nu)$ if $R(t)$ is given over the experimental time interval of 400 nsec by a pure sine wave of twice the Larmor frequency, free of statistical fluctuations. Since there is no observable difference ($<2\times10^{-2}$) between the calculated curve and the experimental data, we conclude that the linewidth of the data is entirely accounted for by the mere fact that we are dealing with the Fourier transform of a truncated sine wave. This, in turn, implies that there can be no damping present in the experimental function $R(t)$, since any damping would broaden the resonance in $F^2(\nu)$ beyond the width observed. From this absence of broadening, we conclude that there are no detectable relaxation processes, i.e., time-dependent perturbations, on the time scale of 400 nsec.

The absence of observable time-dependent perturbations is expected. Far from the critical point, the field fluctuations rate is so rapid that the nuclear spin responds only to the time-average field, and only this average field is detected. On the other hand, close to the critical point, fluctuations slow and increase in amplitude, with both effects having observable consequences on the correlation function. For a randomly jumping field of constant amplitude, Blume[23] has given explicit expressions in all ranges of the fluctuation rate.

It follows, therefore, that if in the fluctuation-insensitive region, far from the critical point, TDPAC linewidths are completely explained in terms of the details of the Fourier analysis, then near the critical point the TDPAC technique ought to be a sensitive probe of the critical fluctuations. The main difficulty in the case of ^{57}Fe would be that there will be an insufficient number of precessions near enough to the critical point. This should not be the case with some other isotopes.

7. COMPARISON WITH MÖSSBAUER EFFECT

Since the Mössbauer effect in ^{57}Fe has been so widely applied, it is interesting to compare TDPAC, as exemplified by the experiment reported here, to the Mössbauer effect.

Some obvious advantages of TDPAC are as follows: (1) The sign of the hyperfine field is easily determined directly from the data, without the need of relatively large external fields, or polarized γ-ray sources. (2) Accuracy is more easily and directly achieved, since crystal clock calibration is trivial compared to an accurate velocity calibration of anything but a lathe-type Mössbauer drive. (3) TDPAC does not depend on recoilless emission, and can be of use where the Mössbauer recoilless fraction becomes negligible, such as, for example, at high temperature, or in certain low Debye-temperature systems.

[23] M. Blume, Ref. 3, p. 911.

Some obvious disadvantages of TDPAC are as follows: (1) It is necessary to prepare a new radioactive source for every study, and, with the unpredictability of diffusion and the expense of ion implantation, this is a considerable factor. (2) Statistical accuracy in TDPAC is more severely restricted than in the Mössbauer effect, since source strengths have an absolute practical limit of $\sim5\ \mu$ Ci, set by permissable accidental background, while Mössbauer source strengths are limited by counter pileup to $\sim10^5$ counts/sec (with special precautions). (3) It is necessary for practical reasons to use polarized sources, as we did, in TDPAC experiments where $A_2\leq0.03$, while Mössbauer experiments can always be done in zero applied field. Zero-applied-field TDPAC experiments are possible, of course, and have been done in cases when the anisotropy is large.[24,25]

A final possible advantage of TDPAC over the Mössbauer effect has to do with fluctuation detection discussed in Sec. 6. For the Mössbauer effect, as in TDPAC, rapid fluctuations produce a response to the time-average field, and slowing fluctuations produce broadening of the line or lines.[23] Yet, for the Mössbauer effect, unlike in the present work, the observed linewidth can rarely be quantitatively accounted for with any precision. One reason for this lies in the details of the resonant absorption process, as discussed by Margulies and Ehrmann,[26] which leads in finite-thickness absorbers to broadening that in practice can easily be as large as 50–100%. In addition, there are often other line broadening effects that are not always easily explained. The effect discussed by Margulies and Ehrmann can be evaluated, but one must know the recoilless fraction, the resonant cross section, and the distribution of resonant atoms in the absorber, as well as the source line shape. Therefore, if a Mössbauer experiment is to be used at all for fluctuation studies, it will be necessary to manipulate the fluctuations while leaving other factors constant, so that the portion of the linewidth due to fluctuations can be identified. For TDPAC, on the other hand, once the full linewidth far from the region of fluctuations has been fully explained, as in this experiment, subsequent line broadening can be wholly attributed to time-dependent perturbations.

ACKNOWLEDGMENTS

For a number of helpful discussions, including some assistance with the fast electronics, we thank S. Berko and A. P. Mills. For a discussion of the fluctuation problem, we thank M. Blume. We also gratefully acknowledge the technical assistance of R. Rosner and B. Werner.

[24] D. A. Shirley, S. S. Rosenblum, and E. Matthias, Ref. 3, p. 480.
[25] J. I. Cisneros, G. Liljegren, T. Lindqvist, and A. Lopez-Garcia, Arkiv Fysik 38, 363 (1968).
[26] S. Margulies and J. R. Ehrmann, Nucl. Instr. Methods 12, 131 (1961).